Dissociative *fac*-to-*mer* photoisomerisation of a Mn(I) tricarbonyl complex containing a highly flexible SPS-based pincer ligand

F. Hartl and T. Mahabiersing

Van't Hoff Institute for Molecular Sciences, University of Amsterdam, Nieuwe Achtergracht 166, 1018 WV Amsterdam, The Netherlands

M. Doux, N. Mézailles and P. Le Floch

Laboratoire "Hétéroéléments et Coordination", UMR CNRS 7653, Département de Chimie, Ecole Polytechnique, 92128 Palaiseau Cédex, France

K. L. Ronayne, M. Towrie and A. W. Parker

Central Laser Facility, STFC, Rutherford Appleton Laboratory, Chilton, Didcot, Oxfordshire, OX11 0QX, UK

Main contact email address   **f.hartl@uva.nl**

Introduction

Terdentate pincer ligands are continuously in the centre of interest due to synthetic and theoretical developments and practical application of their coordination compounds in chemistry of molecular materials and in catalysis. A great variety of *rigid* pincer ligands have been based on 2,6-disubstituted benzene (XCX) and pyridine (XNX), where X's represent chelating side arms with donor C, N, O, P or S heteroatoms [1]. A novel type in this family, an anionic SPS ligand, features a central phosphinine ring with a hypervalent P atom and ancillary phosphine sulfides (Scheme 1). This *highly flexible* pincer ligand has been found to support different coordination geometries, for example square planar and trigonal bipyramidal Rh(I) complexes, with clearly high potential in catalysis. Systematic investigation of the coordination chemistry of the SPS ligand led us to the synthesis of pseudooctahedral complexes *fac*-[M(CO)$_3$(SPS)] (M = Mn(I) and Re(I)] (Scheme 1).
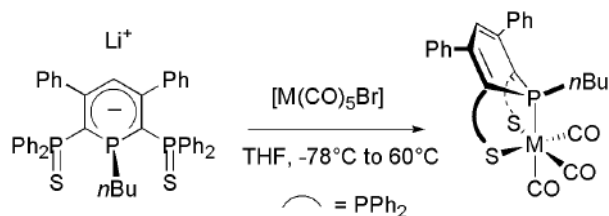
Scheme 1. Molecular structure of the SPS ligand and synthesis of *fac*-[M(CO)$_3$(SPS)] (M = Mn, Re).

In contrast to photostable *fac*-[Re(CO)$_3$(SPS)], the Mn(I) complex undergoes efficient *fac*-to-*mer* photoisoerisation ($\Phi = 0.80\pm0.05$ at $\lambda_{exc} = 460$ nm) upon irradiation into the intense absorption band at 471 nm (Figure 1). A similar, non-solvatochromic, absorption band is displayed by the Re(I) complex and the *mer*-photoproduct. The formation of *mer*-[Mn(CO)$_3$(SPS)] is also evidenced by IR spectroscopy (Figure 2), with changes in the ν(CO) region characteristic for a *fac*-to-*mer* conversion of a tricarbonyl complex.

Owing to the unique coordination properties of the flexible SPS ligand, the meridional conformation of [Mn(CO)$_3$(SPS)] is thermally fairly stable (Figure 2) and could also be characterized by single-crystal X-ray crystallography. Spectro-electrochemistry and DFT calculations have revealed that the frontier (redox)
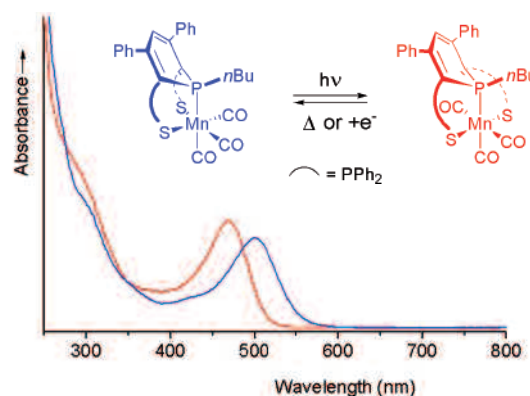
Figure 1. UV-Vis spectra of *fac*-[Mn(CO)$_3$(SPS)] (blue line) and equimolar *mer*-[Mn(CO)$_3$(SPS)] (red line).
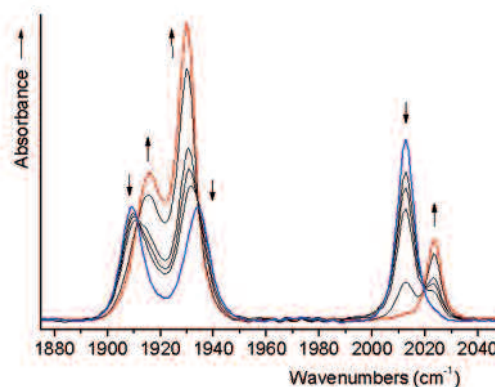
Figure 2. Photoisomerisation of *fac*-[Mn(CO)$_3$(SPS)] (blue line) to *mer*-[Mn(CO)$_3$(SPS)] (red line). The reverse process occurs thermally within ca 8 h in the dark.

molecular orbitals of *fac*- and *mer*-[Mn(CO)$_3$(SPS)] as well as *fac*-[Re(CO)$_3$(SPS)] are largely SPS-based π* orbitals (Figure 3). The intraligand (IL) electronic transition between these orbitals has been shown to contribute dominantly (ca 80%) to the optically allowed lowest-energy electronic absorption in the visible region (Figure 1). The IL Franck-Condon excited state itself, however, cannot be responsible for the photoisomerisation of *fac*-[Mn(CO)$_3$(SPS)]. In addition, *fac*-[Mn(CO)$_3$(SPS)] is much less luminescent ($\lambda_{exc} = 446$ nm, $\lambda_{em} = 566$ nm,

$\Phi_{em} = 5.1 \times 10^{-4}$ in deaerated THF) compared to the *mer*-isomer ($\lambda_{exc} = 446$ nm, $\lambda_{em} = 585$ nm, $\Phi_{em} = 2.5 \times 10^{-3}$ in deaerated THF) and *fac*-[Re(CO)$_3$(SPS)], which points to a reactive excited state quenching the luminescence. The nature of the excited states and early transients involved in the photo-isomerisation pathway was studied by ultrafast time-resolved IR spectroscopy. The Mn–CO bond dissociation was assumed to be the key step in the mechanism, similar to *fac*-to-*mer* photoisomerisation of related complexes *fac*-[MnX(CO)$_3$(α-diimine)] (X = halide)[2].
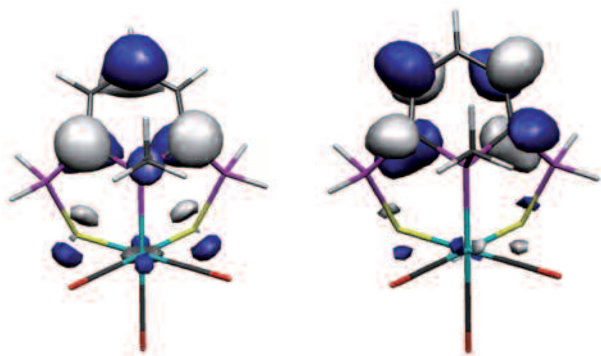

Figure 3. The HOMO (left) and the LUMO (right) of a model complex of *fac*-[Mn(CO)$_3$(SPS)] from G03/B3LYP.

Results and Discussion

The ps-TRIR spectra of *fac*-[Mn(CO)$_3$(SPS)] obtained after 490 nm excitation are shown in Figure 4. The spectra feature bleached ground-state absorptions at 2013, 1932 and 1909 cm^{-1} and transient absorptions at 2048, 1987 and 1970 cm^{-1} (shifted to 2053, 1989 and 1972 cm^{-1} in 7 ps). The significant shift of the ν(CO) bands to higher energy indicates a Mn-to-SPS charge transfer character of the transient excited state (not encountered in the ground-state DFT calculations) or, more likely, a situation where the flexible SPS ligands adopts a conformation that results in decreased Mn-to-CO π-back-bonding. The transient decays in 300 ps and a new species is observed, absorbing at 1943 and 1854 cm^{-1}. At the same time, the ground state is only partially recovered (25%), which nicely corresponds with the photoisomerisation quantum yield (see above). The transient dicarbonyl species **X** was still observed after
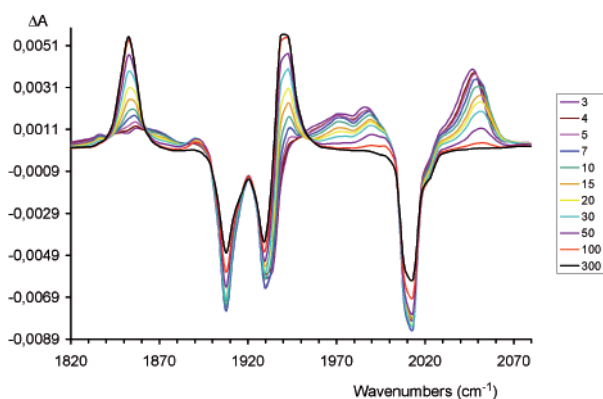

Figure 4. Difference TRIR spectra of *fac*-[Mn(CO)$_3$(SPS)] in THF measured after 490 nm excitation. Time delays are shown in ps. No new bands were observed on the ns time scale.

50 μs. No growth of the ν(CO) bands due to the *mer*-[Mn(CO)$_3$(SPS)] ultimate photoproduct was detected in this time domain. Apparently, the *fac*-to-*mer* isomerisation of *fac*-[Mn(CO)$_3$(SPS)] indeed proceeds via Mn–CO bond dissociation, followed by rearrangement and fairly slow CO recoordination. At the moment we cannot say whether **X** is the only detectable dicarbonyl transient species along the reaction pathway at RT.

Important complementary information has been gained from the ps-TRIR spectra of photostable *fac*-[Re(CO)$_3$(SPS)] in dcm (not shown here). After 490 nm excitation, the picosecond tricarbonyl species absorbing at 2045, ~1989 and ~1975 cm^{-1} (Tr2), which corresponds to the first observable transient in the case of *fac*-[Mn(CO)$_3$(SPS)] (Figure 4), is preceded by another transient (Tr1) absorbing at 2013, ~1931 and ~1908 cm^{-1}. The wavenumbers of Tr1 are close to the bleached ground-state absorption (2015, 1929 and 1896 cm^{-1}). We believe that Tr1 correspond to the initial IL excited state, with the major contribution from the HOMO→LUMO electronic excitation, in agreement with the DFT calculations. The Tr1 absorption completely decays in 50 ps. The Tr2 absorption initially grows within the first 6 ps and then it also decays along with Tr1. At the time delay of 100 ps, only a new tricarbonyl transient Tr3 remains, showing ν(CO) bands (2020, ~1928 and ~1904 cm^{-1}) slightly shifted in comparison with the ground-state wavenumbers. Evidently, we may conclude that the system arrives into another, lower-lying IL excited state. The ground state of *fac*-[Re(CO)$_3$(SPS)] is recovered for ca 50% at this time delay. Tr3 is relatively long-lived, decaying completely within 10 μs, which results in full recovery of the ground state (Figure 5, 355 nm excitation in THF). No dicarbonyl transient was observed in the ps-ns-μs time domain, in line with the photostability of *fac*-[Re(CO)$_3$(SPS)].
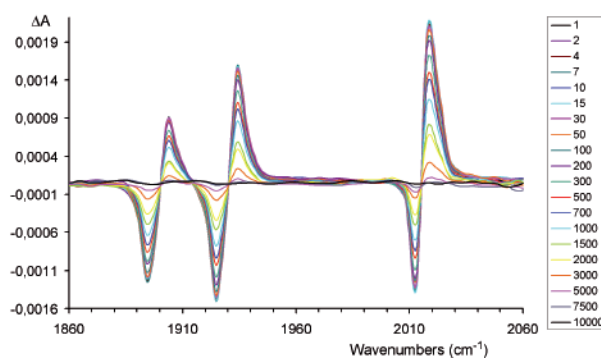

Figure 5. Difference TRIR spectra of *fac*-[Re(CO)$_3$(SPS)] in THF measured after 355 nm excitation. Time delays are shown in ns. The decay corresponds to internal conversion of Tr3 (an SPS-based IL excited state) to the ground state.

The dicarbonyl transient **X** is also formed after 490 nm excitation of *fac*-[Mn(CO)$_3$(SPS)] in THF in the presence of an excess of P(OEt)$_3$. In this case, however, **X** undergoes a conversion on the nanosecond time scale to another species absorbing at 1932 and 1860 cm^{-1}. This process is completed in ca 50 μs. The "trapped" dicarbonyl species, **X**·P(OEt)$_3$ is also formed as a stable compound upon visible irradiation of *fac*-[Mn(CO)$_3$(SPS)] at -90°C in the presence of P(OEt)$_3$. At temperatures above -50°C it

converts to *trans*(CO_{eq},CO_{eq})-[Mn{P(OEt)$_3$}(CO)$_2$(SPS)], the likely monosubstituted analogue of *mer*-[Mn(CO)$_3$(SPS)], showing ν(CO) bands at 1945 and 1877 cm^{-1}. The latter complex was found to convert thermally in about 3.5 h to *cis*(CO_{eq},CO_{eq})-[Mn{P(OEt)$_3$}(CO)$_2$(SPS)], the likely monosubstituted analogue of *fac*-[Mn(CO)$_3$(SPS)], absorbing at 1939 and 1865 cm^{-1}. It is noteworthy that the latter complex cannot be formed directly by a thermal reaction of *fac*-[Mn(CO)$_3$(SPS)] with P(OEt)$_3$ at room temperature.
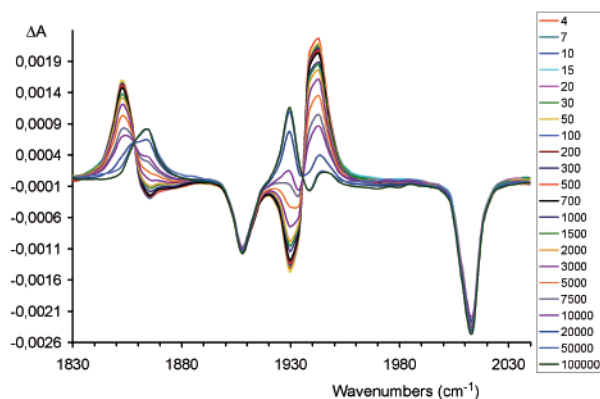
Figure 6. Difference TRIR spectra of *fac*-[Mn(CO)$_3$(SPS)] in THF containing excess P(OEt)$_3$, measured after 355 nm excitation. Time delays are shown in ns. The spectra recorded on the ps time scale correspond to Figure 1.

Conclusions

The above experimental data suggest that the dicarbonyl transient **X** is formed from electronically excited *fac*-[Mn(CO)$_3$(SPS)] by dissociation of an *equatorial* CO ligand, similar to photoreactive complexes *trans*-[MnX(CO)$_3$(α-diimine)] (X = halide) [2]. The molecular structures of **X** and **X**·P(OEt)$_3$ need to be confirmed by quantum chemical calculations. As expected, the ultrafast TRIR experiments have been of key importance for elucidating the photoisomerisation path of *fac*-[Mn(CO)$_3$(SPS)] and the early photochemical dynamics of photostable *fac*-[Re(CO)$_3$(SPS)].

References

1. E. Díez-Barra, J. Guerra, I. López-Solera, S. Meriono, J. Rodríguez-López, P. Sánches-Verdú and J.Tejeda, *Organome-tallics,* **22**, 541, (2003)., and other references cited therein.
2. A. Vlãek Jr., I. R. Farrell, D. J. Liard, P. Matousek, M. Towrie, A. W. Parker, D. C. Grills and M. W. George, *J. Chem. Soc., Dalton Trans.,* **701** (2002).